

Quantitative Investigation of *QRS* Detection Rules Using the MIT/BIH Arrhythmia Database

PATRICK S. HAMILTON AND WILLIS J. TOMPKINS, SENIOR MEMBER, IEEE

Abstract—We have investigated the quantitative effects of a number of common elements of *QRS* detection rules using the MIT/BIH arrhythmia database. A previously developed linear and nonlinear filtering scheme was used to provide input to the *QRS* detector decision section. We used the filtering to preprocess the database. This yielded a set of event vectors produced from *QRS* complexes and noise. After this preprocessing, we tested different decision rules on the event vectors. This step was carried out at processing speeds up to 100 times faster than real time. The role of the decision rule section is to discriminate the *QRS* events from the noise events. We started by optimizing a simple decision rule. Then we developed a progressively more complex decision process for *QRS* detection by adding new detection rules. We implemented and tested a final real-time *QRS* detection algorithm, using the optimized decision rule process. The resulting *QRS* detection algorithm has a sensitivity of 99.69 percent and positive predictivity of 99.77 percent when evaluated with the MIT/BIH arrhythmia database.

INTRODUCTION

SOFTWARE *QRS* detectors are an integral part of modern computerized ECG monitoring systems. Perhaps the most critical use of *QRS* detection occurs in intensive care unit arrhythmia monitoring systems where the algorithm must run in real time. However, there are many other instruments that use such real-time algorithms. These include ECG machines, operating room monitors, and ECG stress test systems. In an arrhythmia monitoring system, significant false negative and false positive rates can result from faulty *QRS* detection [1]. As yet, no one has developed a perfect real-time *QRS* detection algorithm.

Pahlm and Sornmo [2] observe that most *QRS* detectors are divided into two sections. The preprocessor section performs linear and nonlinear filtering of the ECG signal and produces a set of periodic vectors that describe events. The decision rule section operates on the output of the preprocessor, classifies each event as either a *QRS* complex or noise, and saves the temporal location of each of the identified *QRS* complexes.

The decision rules for a *QRS* detector are generally built from a number of components each having experimentally determined parameters. The most important task of the decision rule section is the determination of detection thresholds. Other common components of *QRS* decision

Manuscript received August 28, 1986. This work was supported in part by a grant from the Burdick Division of KONE Instruments, Inc. and the State of Wisconsin Technology Development Fund.

The authors are with the Department of Electrical and Computer Engineering, University of Wisconsin-Madison, Madison, WI 53706.

IEEE Log Number 8611199.

rules are blanking, where events immediately following a *QRS* detection are ignored for a set time, search back, where previously rejected events are reevaluated when a significant time has passed without a detection, and use of slope to distinguish between *T* waves and early occurring ectopic beats.

Decision rule components have generally been assembled in ad hoc fashion. Little has been done to attach quantitative significance to different decision rule components. Fig. 1 shows our experimental approach for examining the effects of different decision rules. We used the preprocessor developed by Pan and Tompkins [3], with slight modifications, to process the MIT/BIH database. The preprocessor produced event vectors consisting of peak heights from the processed ECG signal and time of peak occurrence. These vectors were recorded along with annotation as to whether the event resulted from a *QRS* complex or noise. Progressively more complex decision rules were applied to the event vectors to evaluate the quantitative effects of different decision rule components. At each stage we optimized the decision rules. We implemented the resulting rules in a real-time *QRS* detector together with a derivative algorithm used to discriminate between *T* waves and early ectopic beats.

When designing *QRS* or PVC detectors around a given data set, there is some concern that the detector will be tuned to the database used for development. Small improvements in detector performance on a given database may not reflect significant improvement in real-world performance. Moody and Mark [4] have discussed how well real-world performance can be predicted from performance on a given database. Such performance can only be judged by the clinician with long-term clinical trials. Detection of rare events such as ventricular tachycardia and the effects of noise under different conditions cannot be accurately judged with limited databases. The general consensus is that databases such as the MIT/BIH yield the best indication of arrhythmia detector performance available without extensive clinical trials.

PREPROCESSOR

The preprocessor does linear and nonlinear digital filtering and peak detection.

Filtering

Fig. 2 illustrates the filter stages of the preprocessor. See Pan and Tompkins [3] for further details. The low-

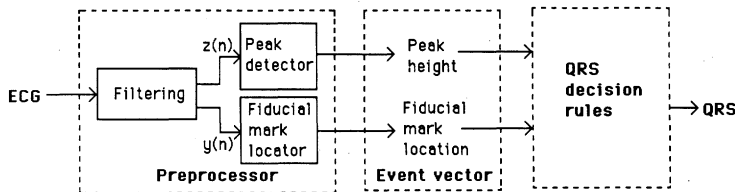


Fig. 1. Block diagram of *QRS* detector algorithm. The preprocessor does linear and nonlinear digital filtering and peak analysis to produce event vectors. The vectors are processed by decision rules to locate *QRS* complexes.

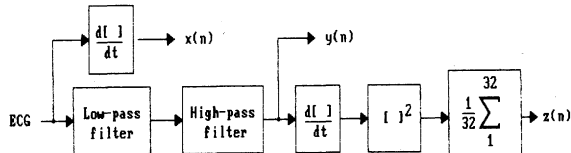


Fig. 2. Filter stages of the *QRS* detector. $z(n)$ is the time-averaged signal, $y(n)$ is the bandpassed ECG, and $x(n)$ is the differentiated ECG.

pass and high-pass filters together form a bandpass filter that can be implemented with integer arithmetic to provide for real-time operation. This is followed by differentiation, squaring, and time averaging of the signal. A separate derivative of the original ECG is used for *T* wave discrimination.

The low-pass filter is one of a class of filters described by Lynn [5], implemented with the difference equation

$$\begin{aligned} y(nT) &= 2y(nT - T) - y(nT - 2T) + x(nT) \\ &\quad - 2x(nT - 6T) + x(nT - 12T) \end{aligned}$$

where T is the sampling period and n is an arbitrary integer. The high-pass filter is implemented with the difference equation

$$\begin{aligned} y(nT) &= y(nT - T) - x(nT)/32 + x(nT - 16T) \\ &\quad - x(nT - 17T) + x(nT - 32T)/32. \end{aligned}$$

The difference equation for the derivative is

$$\begin{aligned} y(nT) &= (2x(nT) + x(nT - T) \\ &\quad - x(nT - 3T) - 2x(nT - 4T))/8. \end{aligned}$$

The nonlinear squaring function squares each output data point. Time averaging is done by adding together the 32 most recent values from the squaring function and dividing the total by 32.

Fig. 3 shows a typical ECG and the resulting output signals after each of the processing steps.

Peak Detection

Fig. 4 shows a typical large waveform produced by the time-averaged window for a *QRS* complex. Although it is easy to visually identify one large peak, simple peak detection algorithms falsely detect multiple peaks due to ripples in the wave. A simple local maxima peak detector has the liability of detecting many small-amplitude peaks. Although both peaks result from the same *QRS* complex, one peak is classified as resulting from a *QRS* complex,

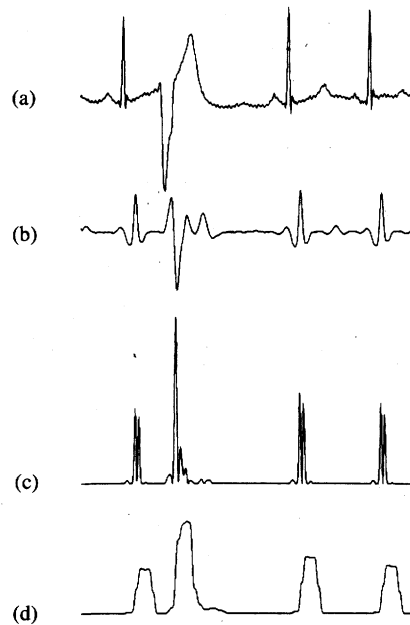


Fig. 3. Outputs of filters in the *QRS* detector. (a) Unfiltered ECG. (b) Output of bandpass filter. (c) Output after the bandpass, differentiation, and squaring processes. (d) Final time-averaged signal.

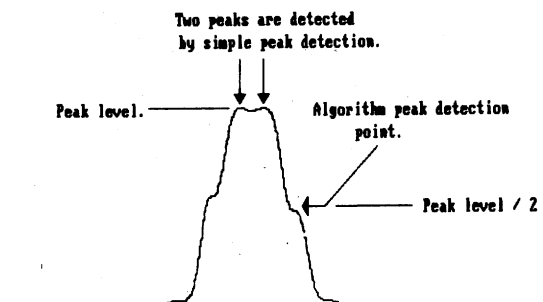


Fig. 4. Typical waveform of time-averaged signal during the *QRS* complex.

the other is classified as noise. This can bias the noise level estimate on the high side. In contrast, ripples in the baseline of the signal can bias the noise estimate on the low side.

Murthy and Rangaraj [6] proposed a time-averaged, first difference signal having somewhat similar characteristics to our bandpassed, differentiated, squared, time-averaged signal. They advocated low-pass filtering of the time-averaged signal to reduce ripples and multiple peaks before peak detection. However, instead of adding such an additional filter stage, we developed a peak detection al-

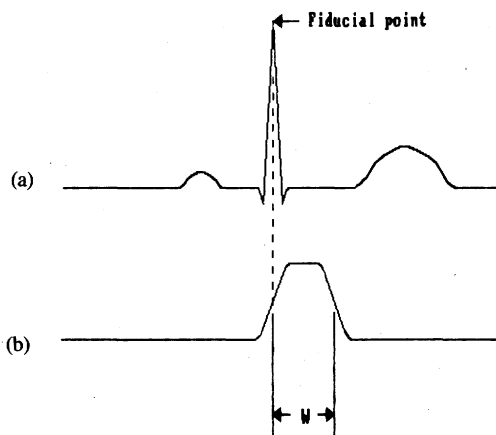


Fig. 5. Idealized relationship between the *QRS* complex and the time-averaged waveform. (a) Unfiltered ECG. (b) Time-averaged signal. Interval *W* equals the width of the averaging window.

gorithm that eliminates detection of both ripples on large waves and also very small noise peaks.

The peak detector finds peaks in the final output of the filtering stages. A detected peak defines an event. The detector algorithm stores the maximal levels encountered in the signal since the last peak detection. A new peak is defined only after a level is encountered that is less than half the height of the maximal, or peak, level. Detection occurs halfway down the back side of the peak. This approach eliminates multiple detections from ripple around the wave peak.

When ECG signals have prominent *T* waves, the time-averaged waveform for a heart cycle sometimes appears as one long wave formed from the combination of waves produced by the *QRS* complex and the *T* wave. The time of occurrence of the peak detected in the preprocessed signal is important for placing the fiducial mark. With a prominent *T* wave, the detection may be delayed by the duration of the lengthened wave. To avoid this delay, in addition to the previously stated conditions for detection, a *QRS* is detected by the peak detector if 175 ms elapses from the occurrence of the maximal positive slope in the time-averaged signal. The reasons for this detection condition will become clearer to the reader later in the discussion on the fiducial mark.

FIDUCIAL MARK

Fig. 5 shows an idealized relation between the *QRS* complex and the time-averaged signal. The peak of the *R* wave occurs in the middle of the rising slope of the time-averaged signal. As already discussed, the peak detection algorithm does not establish that a valid peak has occurred until the middle of the falling slope when the level drops below half the distance from the maximal value to the base point. Because the time between the middle of the rising slope and the middle of the falling slope is equal to the duration of the averaging window, ideally the fiducial mark representing the time of occurrence of the peak of the *R* wave is located with a fixed delay of one window's

width (i.e., 160 ms) back in time from the point of peak detection.

For a more consistent location, the fiducial mark is set to the location of the largest peak in the bandpassed signal in an interval from 225 to 125 ms preceding a peak detection in the time-averaged signal. We use peaks in the signal from the bandpass filter only for location of the fiducial mark, so a simple three-point scheme is used for detection of peaks in this signal. To compensate for late detection, when a peak detection occurs with a long wave in the bandpassed signal, the valid fiducial interval is from 250 to 150 ms preceding the peak detection.

DECISION RULE OPTIMIZATION

We preprocessed all the MIT/BIH tapes with the filters and peak detector. For each detected peak, we determined and saved a two-dimensional event vector composed of the peak signal level of the preprocessed waveform and the elapsed time from the last fiducial mark. We also saved a flag that notes whether the vector resulted from noise or from a *QRS* complex. All the event vectors for the entire database require about 700 kbytes for storage. We used these digital recordings of the event vectors to optimize the decision rules. Even with complicated decision rule schemes, we were able to run as many as 100 trials on an IBM PC in the time required for one real-time analysis of the entire set of analog tapes in the database.

We analyzed the effects of different parts of the decision rule stage by constructing and testing an increasingly complex decision rule scheme. As we added new rules, we varied their parameters along with detection threshold parameters to produce optimal performance. Initially we examined different peak level estimation schemes and set the detection threshold as a percentage of the *QRS* peak level estimate. After determining the best method for estimating peak levels, we applied the method to a scheme where the detection threshold is set between the noise level estimate and the *QRS* peak level estimate. Next, we introduced 200 ms refractory blanking to eliminate both false detection on the *T* wave and also multiple detection of the *QRS* complex. Finally, we introduced search back and optimized the relative search back and normal thresholds.

QRS detectors may be optimized with respect to the number of false positive and false negative detections. The relative cost of false detections varies from application to application. Thakor *et al.* [7] used receiver operating characteristic (ROC) curves to analyze the performance of *QRS* detectors. They chose the "knee" of each curve as the point of optimal detector performance. If the probability of a noise occurrence and the probability of a *QRS* occurrence are approximately the same, then a detector operating at the optimal or "knee" point will produce the minimal total number of false positive and false negative detections. In our case, we optimized the decision rules for *QRS* detection to minimize the sum of false negative and false positive detections.

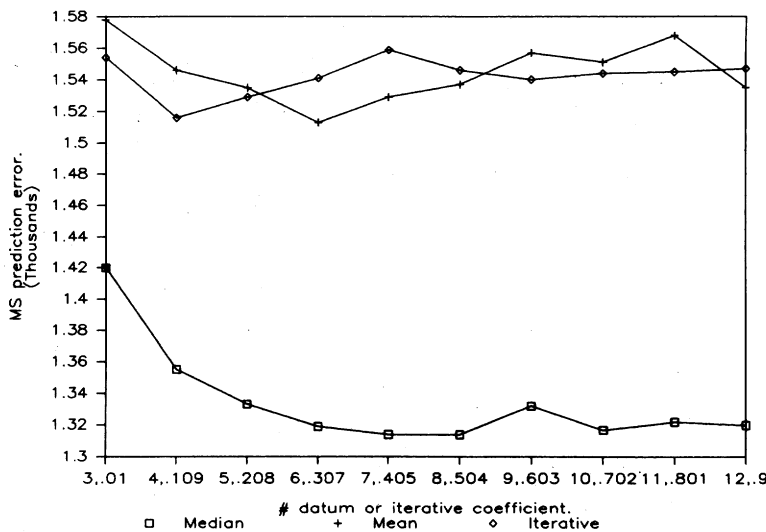


Fig. 6. Mean square prediction error for the mean, median, and iterative signal peak estimators applied to the time-averaged signal.

PEAK LEVEL ESTIMATION

The method of local peak level estimation is an important performance factor in the *QRS* detection algorithms that use adaptive detection thresholds. We examined the relative performance of mean, median, and iterative peak level estimators. The mean estimator determines the local peak level as the mean of a specified number of past peaks whereas the median estimator uses the median peak level. The first-order iterative estimator has the general form

$$\begin{aligned} \text{Estimate}(n) &= (1 - A) \times \text{Estimate}(n - 1) \\ &\quad + A \times \text{Peak}(n) \end{aligned}$$

where A is a positive coefficient less than one.

Mean Square Prediction Error

The peak level estimator may also be considered a predictor, predicting the value of the next *QRS* peak based on the previous *QRS* peaks. If the estimator were perfect, the detection threshold could be set just below the predicted peak level. We applied the three estimators to the peaks derived from the time-averaged signal and tabulated the mean square prediction errors. For the mean and median estimators, we performed trials with different numbers of data points used in the calculation of the peak level estimate. For the iterative estimator, we did trials with ten coefficient values ranging from 0.01 to 0.9.

Fig. 6 illustrates the relative performance of the three predictors applied to *QRS* peaks. The median predictor has a lower prediction error than either the mean or iterative predictor. Its minimal error occurs when seven or eight previous data points are used for level prediction. The performance of the mean and iterative predictors is about equal.

Fig. 7 shows the performance of the mean and median predictors as applied to the noise peaks of the bandpassed signal. The iterative predictor is not shown because its mean square prediction error is generally much larger than

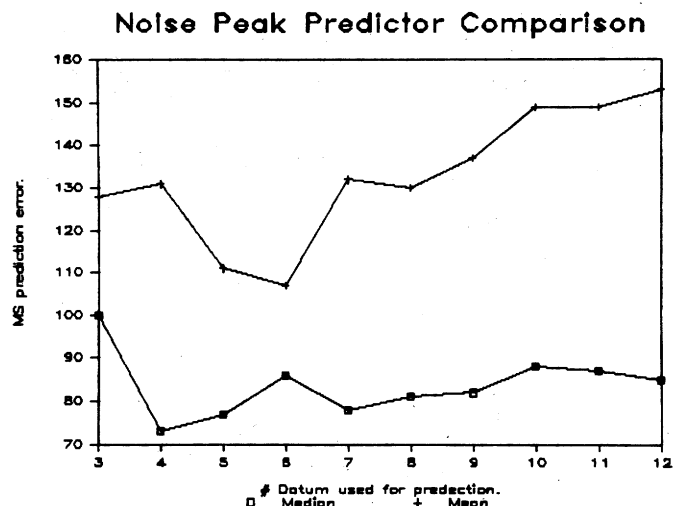


Fig. 7. Mean square prediction error for the mean and median noise peak estimators applied to the time-averaged signal. Most trials of the iterative estimator had too large an error to plot on this scale.

the other two for the range of coefficient values that we tested. For example, with a coefficient of 0.5044, the iterative predictor produced a mean square prediction error of 3116. However, a coefficient of 0.9 reduced the error to only 93.

As with the *QRS* peaks, the median predictor appears to be the best predictor of noise peaks, producing a minimal mean square error using only four data points. However, it is possible that iterative predictors with coefficients higher than 0.9 could do better.

Peak Estimator Performance

For our application, the ultimate performance measure of a peak estimator is its effect on *QRS* detection. One estimator may yield a consistently low peak prediction, and another with a better mean square error might give inconsistent predictions. The consistent predictor is preferable because it will produce fewer false positive and

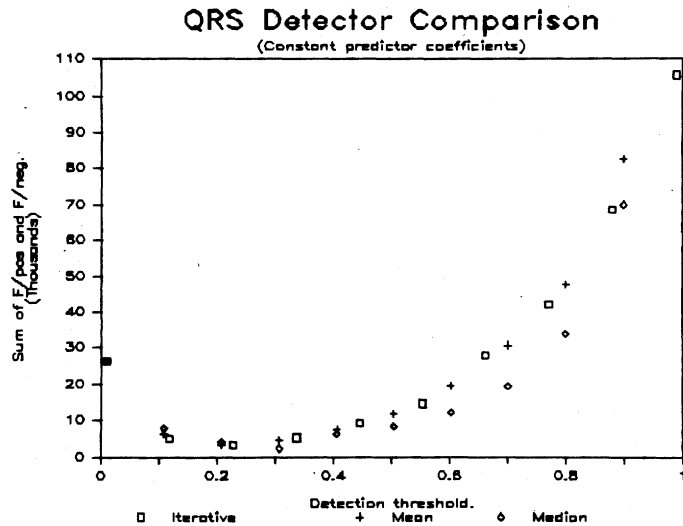


Fig. 8. False detections as a function of detection threshold level for *QRS* detectors based on mean, median, and iterative estimators.

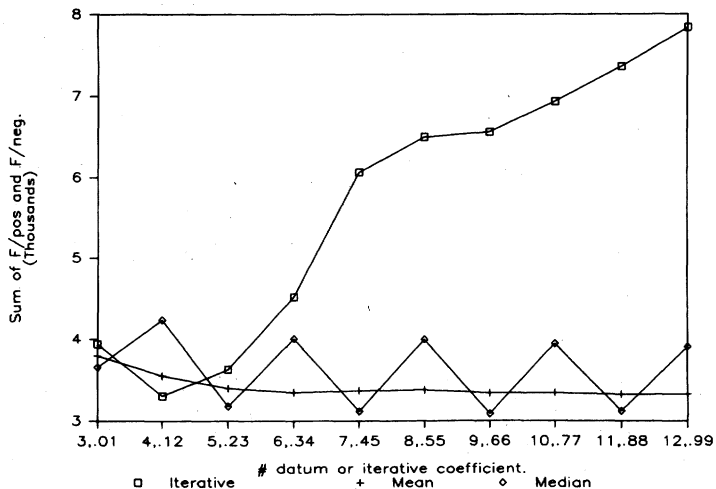


Fig. 9. False detections for *QRS* detectors as a function of parameter changes of the mean, median, and iterative predictors. The mean and median predictors are plotted as a function of the number of data points in the calculation. The iterative predictor coefficients are shown.

false negative detections if the proper relative detection threshold is used.

We tested a simple *QRS* detector to compare peak level estimator performance. We set the detection threshold to be a percentage of the *QRS* peak level estimate.

$$\text{Detection threshold} = B \times \text{Peak level estimate.}$$

The detection threshold coefficient B is set to values between zero and one. Any peaks larger than the detection threshold are classified as *QRS* complexes and are used to update the detection threshold. Noise peaks are ignored.

We performed trials with mean, median, and iterative peak level estimators. For the mean and median estimators, we varied both the detection threshold coefficient B and also the number of data points used for estimation. For the iterative estimator, we varied both the iterative coefficient and also the detection threshold, each throughout the range from 0.01 to 0.99. In our initial trials

of the mean and the median estimators, we used ten different groups of 3–12 data points. We applied ten detection threshold coefficient levels ranging from 0.01 to 0.9 for a total of 100 trials. We did a second set of trials using thresholds approximately equal to those that performed best in these first trials.

Fig. 8 shows the general performance of the three *QRS* detectors as a function of the detection threshold level. For each estimator, the sum of the false negative and false positive detections is plotted as a function of the detection threshold. The median estimator provided the minimal number of false detections and fewer false detections than the others for most of the detection threshold range. In general, all the *QRS* detectors work best with detection threshold coefficients between 0.15 and 0.4.

Fig. 9 illustrates the performance of the three *QRS* detectors tested with similar detection threshold coefficients. The *QRS* detectors with the mean and median peak

200 ms Blanking Performance Comparison

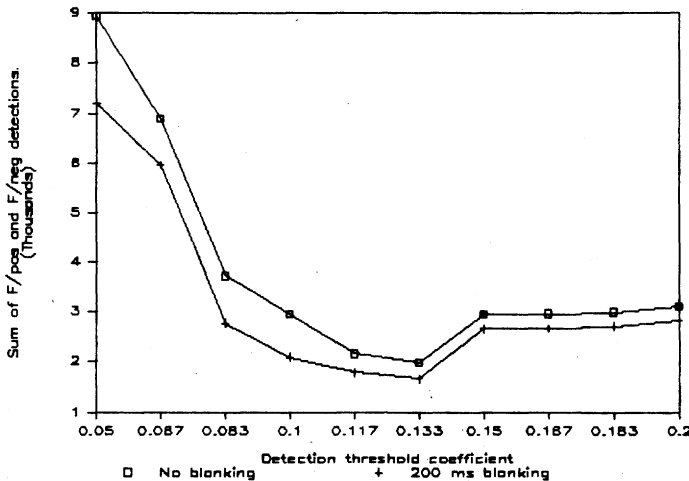


Fig. 10. Influence of blanking on false detections for a *QRS* detector with a median peak level estimator.

level estimators have detection threshold coefficients of 0.208. The *QRS* detector with the iterative estimator has a detection threshold of 0.228. The iterative estimator works best with an iterative coefficient of 0.119, and its performance deteriorates for larger iterative coefficients. The performance of the mean estimator improves slightly as more data points are used for estimation. The median estimator oscillates with odd and even numbers of data points used in the median, but tends to improve with larger numbers of data points. This oscillation probably results because we chose the lower of the middle two numbers to be the median for an even number of data points. Thus, statistically, the median of an even number of data points produces a lower estimate than the median of an odd number of points. With a detection coefficient of 0.208, the median estimators using an odd number of data points perform better than those using an even number. For a detection coefficient of 0.307, the performance switches, such that the even-median estimators are better.

We performed a second set of trials to determine the number of data points and coefficients for each estimator that produce the fewest number of false detections. The iterative estimator has a minimum of 2564 false detections when using an estimator coefficient of 0.043 with a detection threshold coefficient of 0.211. The mean estimator has a minimum of 3147 false detections using 15 data points in the mean and a detection threshold coefficient of 0.167. Although it is possible that using more than 15 points for the mean would improve performance, we did not test this possibility. The median estimator produces the minimal number of false detections of the three techniques with 2088 false detections for a median of 12 data points and a detection threshold coefficient of 0.283.

The median estimator performs better than either the mean or iterative estimator as a predictor of peak levels for both *QRS* and noise and as a peak level estimator for *QRS* detection. Therefore, we used the median estimator in all the following *QRS* detector trials.

DETECTION THRESHOLD

In our tests of peak level estimators, we used a simple detection threshold scheme which relied only on the *QRS* peak level estimate. Both *QRS* peak and noise peak level estimates may be used to determine the detection threshold. The threshold equation

$$DT = NPL + TC \times (NPL - QRSPL) \quad (1)$$

has been used [3] where *DT* is the detection threshold, *NPL* is the noise peak level, *TC* is the threshold coefficient, and *QRSPL* is the *QRS* peak level. We tested this method for calculating detection thresholds with median peak level estimators. Prediction performance of the median estimator for noise and *QRS* peaks was similar, so we used the same number of data points for calculating both.

We performed trials with peak estimators using from 3 to 12 previous-peak data points and detection threshold coefficients from 0.01 to 0.9. A *QRS* detector with a 10 data-point median and a detection threshold of 0.133 gave the minimal number of 1974 false detections.

Some improvement can be obtained by including a noise peak estimate in calculation of detection threshold, but the median estimator must be adjusted or only very slight improvement is made in the overall *QRS* detection. The adjustment to the estimator is probably a compromise between the optimal number of data points for noise peak estimation and the optimal number needed for *QRS* peak estimation. Ideally, different estimators might be used for noise and *QRS* peaks. For simplicity, in the following *QRS* detection trials, we used the same estimator for noise and *QRS* estimation.

REFRACTORY BLANKING

After a *QRS* complex occurs, there is a physiological refractory period of about 200 ms before another can occur. Fig. 10 shows that the performance of a *QRS* detector with median peak level estimation and a threshold be-

RR Predictor Comparison

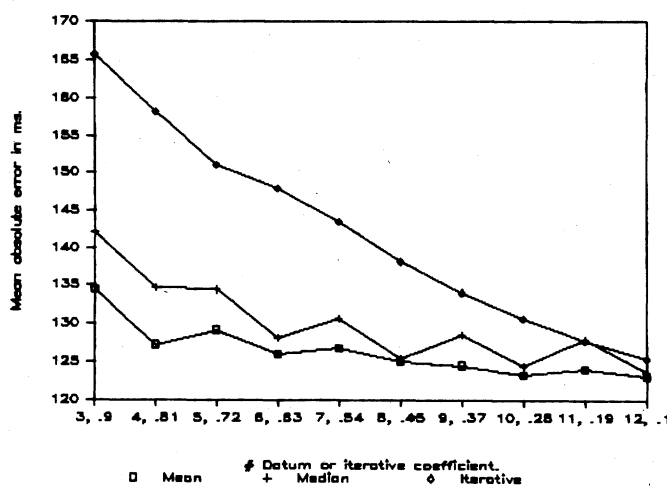


Fig. 11. Performance of *RR* interval predictors based on mean, median, and iterative estimators.

tween the noise and peak estimate is improved for all threshold levels when 200 ms blanking is used. A minimal number of false detections of 1622 was obtained with an eight-point median and a threshold coefficient of 0.133.

SEARCH BACK

Optimization of the search back feature requires analysis of *RR* interval prediction and the relative levels of the normal and search back detection thresholds.

RR Interval Prediction

As with the peak level estimator, we examined mean, median, and iterative prediction of the *RR* interval. Fig. 11 shows the relative performance of the three methods. The mean absolute prediction errors of the three *RR* predictors are plotted as functions of the number of data points or the iterative coefficient used for prediction. For all values, the mean predictor has a smaller prediction error than either the median or iterative predictor, but the performance of all the predictors is comparable for large numbers of data points and small iterative coefficients.

Chernoff *et al.* [8] examined the mean predictor and the iterative predictor in the context of beat classification. They tested mean (or moving average) predictors on the MIT/BIH database with 1-6 data points used for prediction calculation. They tested iterative predictors with coefficients of 0.1, 0.3, and 0.5. They concluded that the iterative method performs better than the mean method of *RR* interval prediction. These results agree with ours, but do not go far enough toward our conclusion that the mean predictor performs better than the iterative when more than six data points are used.

The median and mean predictors perform comparably when using eight data points in the median. Thus, we used the median predictor with eight data points in subsequent search back testing.

Search Back Detection Threshold

We examined the effect of relative normal and search back thresholds on *QRS* detection. The *QRS* detector used eight-point median peak level estimators, a detection threshold calculated according to (1), a 200 ms refractory period, and a median *RR* interval predictor. If no *QRS* complex was detected within 150 percent of the latest *RR* interval, then we applied the search back detection threshold to the peaks previously classified as noise in that range.

We tried two methods of calculating the search back threshold. One method used a new threshold coefficient. The other calculated the search back threshold as a percentage of the normal detection threshold. For the first method we did trials with ten values for the normal threshold coefficient from 0.1 to 0.5. We tested ten levels of search back detection coefficients from 0.01 to 0.1 for each normal threshold coefficient. With the second method we used the same normal coefficients but varied search back thresholds from 0.05 to 0.5 times the normal threshold.

Both methods of calculating the search back detection threshold yielded a minimum of 1422 false detections. The first method produced the minimum with a normal threshold coefficient of 0.189 and a search back detection threshold coefficient of 0.02. The second method produced the minimum with the same normal threshold and a search back threshold 0.3 times the normal.

DISCUSSION

More complete algorithm testing can be done with more information from the preprocessor stage. Practical constraints limited us to the recording of levels and arrival times of peaks from the time-averaged signal. More complete testing would include all factors used by the Assembly language algorithm decision rule, peak values of the bandpassed signal, and maximal derivative values as well as the peak values of the time-averaged signal and fiducial point arrival times. Experiments could show whether or not performance can be improved by using peak data from the bandpassed signal.

Fig. 12 summarizes the quantitative effect of different decision rule components on *QRS* detection. The total false detections are shown for the optimal performance of different stages of *QRS* detector development. Of greatest importance is the selection of a peak level estimator. Including the noise peak estimate in the calculation of the detection threshold results in only a small performance improvement. The addition of 200 ms of refractory blanking contributes more to the algorithm's performance than the introduction of search back. The effects of the different sections on performance are probably not independent. We suspect that details of the algorithm such as search back may be able to compensate for suboptimal performance of other algorithm factors. It is even possible that poorer estimators might yield better detector performance when other algorithm improvements are added.

QRS Detector Performance

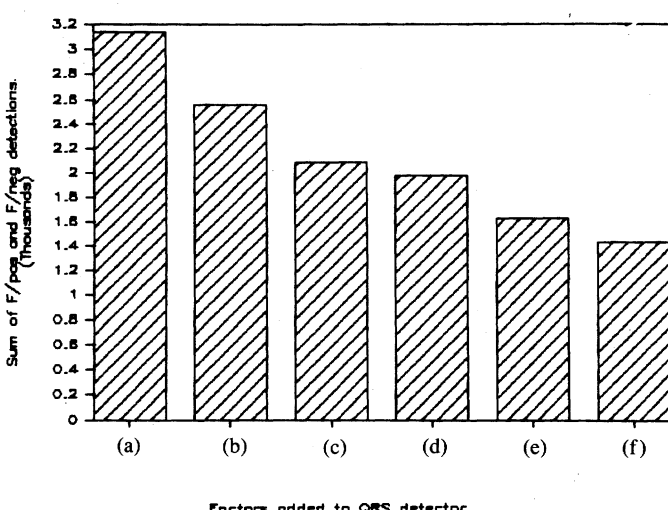


Fig. 12. Influence of processing techniques on performance of the *QRS* detector. (a) Iterative peak level estimator. (b) Mean peak level estimator. (c) Median peak level estimator. (d) Detection threshold that includes the noise peak estimate. (e) 200 ms refractory blanking. (f) Search back.

Further tests could establish the relative independence of different algorithm components.

REAL-TIME IMPLEMENTATION

We implemented the final optimized *QRS* detection algorithm in real time with the C language. The decision rule section uses an eight-point median peak level estimator, a detection threshold coefficient of 0.1825, a search back threshold of half the normal threshold, an eight-point median *RR* interval estimator, and a 200 ms refractory blanking period. Although the best detector tested had a normal threshold coefficient of 0.189, not 0.1825, and a search back threshold 30 percent of the normal detection threshold rather than 50 percent, we chose coefficients for this real-time implementation that are easily calculated with power-of-two arithmetic. We also added to the real-time implementation the maximal derivative for *T*-wave discrimination. The *T*-wave discriminator rejects any detections between 200 and 360 ms following a *QRS* detection, unless the complex has a maximal derivative in its unfiltered ECG greater than half that of the previous *QRS*.

QRS DETECTOR PERFORMANCE

Table I lists the tape-by-tape performance of the new *QRS* detector on the MIT/BIH database. The detector produces 340 false negative detections and 248 false positive detections for a sensitivity of 99.69 percent and a positive predictivity of 99.77 percent. This excludes episodes of ventricular flutter that occur on tape 207.

SUMMARY

We used the MIT/BIH arrhythmia database to quantitatively examine relative importance of commonly used *QRS* detection decision rules. We concluded that the *QRS*

TABLE I
RESULTS OF REAL-TIME EVALUATION WITH QDES SYSTEM

Tape (#)	Total (beats)	FP	FN	Failed detection (FP + FN)	Failed detection (FP + FN)/Total
100	2267	2	0	2	0.09
101	1859	3	1	4	0.22
102	2181	0	0	0	0.00
103	2081	0	1	1	0.05
104	2224	3	7	10	0.45
105	2564	53	22	75	2.95
106	2024	1	2	3	0.15
107	2131	0	3	3	0.14
108	1757	50	47	97	5.67
109	2526	0	1	1	0.04
111	2120	3	2	5	0.24
112	2536	0	0	0	0.00
113	1791	2	1	3	0.17
114	1872	5	7	12	0.64
115	1945	0	0	0	0.00
116	2409	4	25	29	1.22
117	1532	10	3	13	0.85
118	2273	2	2	4	0.18
119	1985	2	0	2	0.10
121	1858	1	0	1	0.05
122	2471	0	0	0	0.00
123	1514	0	0	0	0.00
124	1613	0	0	0	0.00
200	2595	3	2	5	0.19
201	1946	3	19	22	1.14
202	2134	0	0	0	0.00
203	2976	14	61	75	2.57
205	2650	1	4	5	0.19
207*	1856	5	5	10	0.54
208	2953	9	19	28	0.95
209	2999	2	2	4	0.13
210	2645	2	41	43	1.65
212	2746	0	0	0	0.00
213	3245	0	1	1	0.03
214	2255	2	4	6	0.27
215	3357	0	0	0	0.00
217	2202	2	4	6	0.27
219	2150	1	1	2	0.09
220	2041	0	0	0	0.00
221	2422	1	1	2	0.08
222	2492	40	37	77	3.14
223	2603	0	2	2	0.08
228	2048	19	6	25	1.22
230	2252	0	1	1	0.04
231	1566	0	0	0	0.00
232	1719	3	0	3	0.10
233	3135	0	3	3	0.10
234	2747	0	0	0	0.00
TOTALS:		109267	248	340	588
0.54					

* Episodes of ventricular flutter excluded from counts.

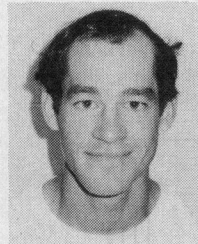
peak estimation component of the *QRS* detector is of primary importance, with a median estimator performing better than either iterative or mean peak estimators. Based on the experimental studies, we developed a real-time *QRS* detection algorithm in the C language from the optimized set of decision rules together with added *T*-wave discrimination. The *QRS* detection algorithm uses integer arithmetic, making it particularly suitable for real-time implementation. The algorithm's performance is comparable to other algorithms evaluated with the MIT/BIH database. Extensive clinical testing would be required of all available algorithms to differentiate significant performance differences between this one and others.

REFERENCES

- [1] C. Zeelenberg and S. H. Meij, "Evaluation and optimization of an existing arrhythmia detection system by using an annotated ECG database," *Comput. Cardiol.*, pp. 103-108, 1981.
- [2] O. Pahlm and L. Sornmo, "Software *QRS* detection in ambulatory monitoring—A review," *Med. Biol. Eng. Comput.*, vol. 22, pp. 289-297, 1984.
- [3] J. Pan and W. J. Tompkins, "A real-time *QRS* detection algorithm," *IEEE Trans. Biomed. Eng.*, vol. BME-32, no. 3, pp. 230-236, 1985.
- [4] G. Moody and R. Mark, "How can we predict real-world performance of an arrhythmia detector," *Comput. Cardiol.*, pp. 71-76, 1983.
- [5] P. A. Lynn, "Online digital filters for biological signals: Some fast designs for a small computer," *Med. Biol. Eng. Comput.*, vol. 15, pp. 534-540, 1977.
- [6] I. S. N. Murthy and M. R. Rangaraj, "New concepts for PVC detection," *IEEE Trans. Biomed. Eng.*, vol. BME-26, no. 7, pp. 409-416, 1979.
- [7] N. V. Thakor, J. G. Webster, and W. J. Tompkins, "Optimal *QRS* detector," *Med. Biol. Eng. Comput.*, vol. 21, pp. 343-350, 1983.

- [8] D. Chernoff, T. Lee, G. Moody, and R. Mark, "Evaluation of *R-R* interval predictors using an annotated ECG database," *Comput. Cardiol.*, pp. 359-362, 1981.

Willis J. Tompkins (S'61-M'66-SM'77), for a photograph and biography, see this issue p. 1140.



Patrick S. Hamilton received the B.S. degree in electrical engineering from the Massachusetts Institute of Technology, Cambridge, in 1981, and the M.S. degree in biomedical engineering from the University of Wisconsin-Madison, in 1985.

He has worked as a Design Engineer for Analogic Corporation, Wakefield, MA, and as a Staff Engineer in the M.I.T. Laboratory for Medical Ultrasonics. In his spare time he is working towards the Ph.D. degree in electrical engineering at the University of Wisconsin-Madison. His research interests include computerized arrhythmia analysis and biomedical signal processing.

SEARCHED _____
INDEXED _____
SERIALIZED _____
FILED _____
JULY 13 1987
FBI - MILWAUKEE

SEARCHED _____
INDEXED _____
SERIALIZED _____
FILED _____
JULY 13 1987
FBI - MILWAUKEE

SEARCHED _____
INDEXED _____
SERIALIZED _____
FILED _____
JULY 13 1987
FBI - MILWAUKEE

ACKNOWLEDGMENT

We thank Dr. John P. Kellman for his support and encouragement during this work. We also thank Dr. Michael J. Coughlin for his useful comments on this paper. This work was supported by grants from the National Institutes of Health (NIH) and the National Science Foundation (NSF). One of us (P.S.H.) was supported by a fellowship from the American Heart Association. This work was partially funded by the U.S. Army Research Institute of Environmental Medicine (ARIEM) and the Defense Advanced Research Projects Agency (DARPA). The authors would like to thank the anonymous reviewers for their valuable comments and suggestions.

Correspondence to: Patrick S. Hamilton, Department of Electrical Engineering, University of Wisconsin-Madison, 440 N. Charter Street, Madison, WI 53706.

Manuscript submitted April 1987; revised June 1988. This work was partially funded by the Defense Advanced Research Projects Agency (DARPA) under contract AF-85-1030. The views expressed in this paper are those of the authors and do not necessarily reflect the position or policy of DARPA or the U.S. Government.

© 1989 IEEE. Reprinted with permission from *IEEE Transactions on Biomedical Engineering*, Vol. 36, No. 8, August 1989, pp. 1161-1169. The original document is available via IEEE Xplore or through your institution's library.